Electronic Supplementary Material (ESI) for Biomaterials Science.
This journal is © The Royal Society of Chemistry 2019

Supporting Information

A Cascade-Reaction Enabled Synergistic Cancer Starvation/ROS-mediated/chemo-Therapy with Enzyme Modified Fe-based MOF

Zongjun Liu, Tuo Li, Fang Han, You Wang, Yang Gan,* Junhui Shi, Tianran Wang, Muhammad Luqman Akhtar, and Yu Li.**

Z. Liu, T. Li, J. Shi, Prof. Y. Wang
School of Materials Science and Engineering
Harbin Institute of Technology, Harbin 150001, China.
E-mail: y-wang@hit.edu.cn

Z. Liu, Prof. Y. Gan
School of Chemistry and Chemical Engineering
Harbin Institute of Technology, Harbin 150001, China.
E-mail: ygan@hit.edu.cn

Prof. F. Han, T. Wang, M. L. Akhtar, Prof. Y.Li
School of Life Science and Technology
Harbin Institute of Technology, Harbin 150001, China.
E-mail: liyugene@hit.edu.cn

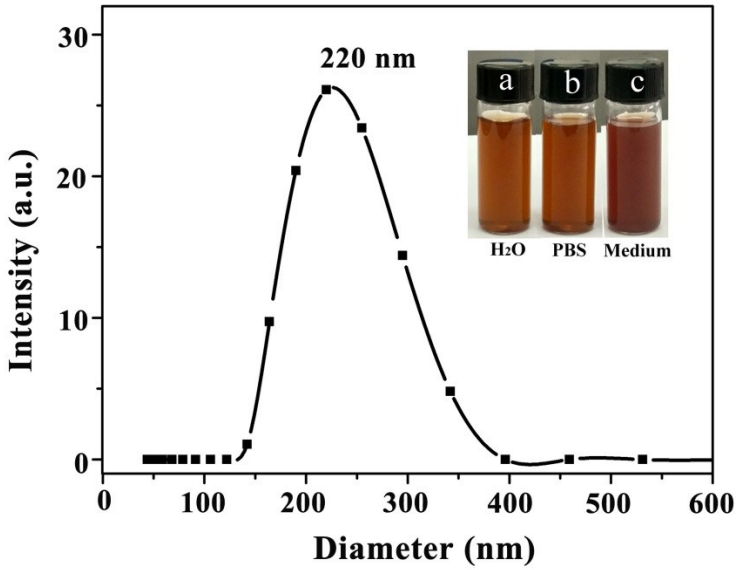

Figure S1. Dynamic light scattering (DLS) measurement of MOF(Fe) particles in water. The average particle size of MOF(Fe) is 220 nm, which is basically in agreement with TEM and SEM data as shown in Figure 1. This result indicates that the as-prepared MOF(Fe) particles are well dispersed in water without detectable aggregation. Insets are the photographs of stable dispersions of MOF(Fe) in different solvents for 12 h incubation: (a) H_2O; (b) PBS; (c) DMEM supplied with 10% FBS.

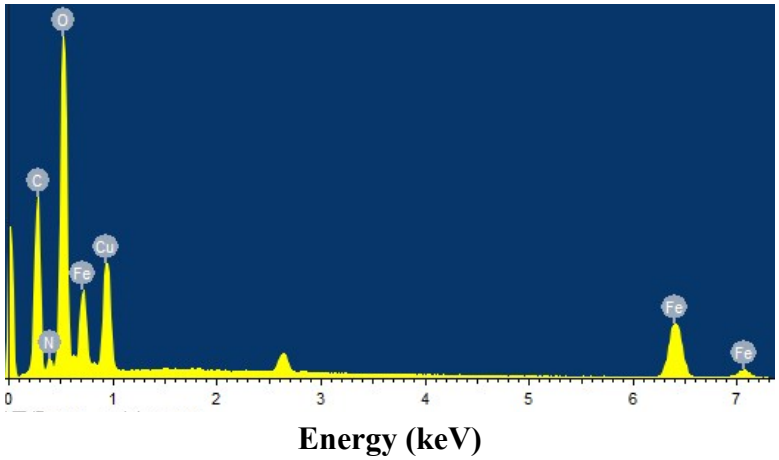

Figure S2. Energy-dispersive X-ray spectroscope (EDS) spectrum of MOF(Fe). These MOF(Fe) were synthesized by heating the solution of aminoterephthalic acid (BDC) and $FeCl_3$ under microwave irradiation. Elements C, N, O and Fe can be seen in this graph, which are originated from BDC ($C_8H_7NO_4$) and $FeCl_3$ respectively. The detection of C, N, O and Fe element indicates a successful preparation of Fe-based MOF. Note that the detected Cu element comes from the copper substrate for depositing MOF(Fe) samples. The peak at 2.6 keV is due to Cl element from $FeCl_3$.[1, 2]

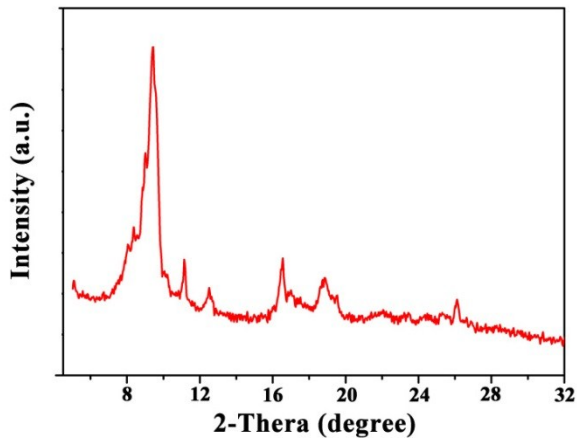

Figure S3. X-Ray diffraction pattern of MOF(Fe). The powder XRD pattern is in accordance with the data reported in literature,[3] indicating a successful preparation of MIL-101(Fe) material.

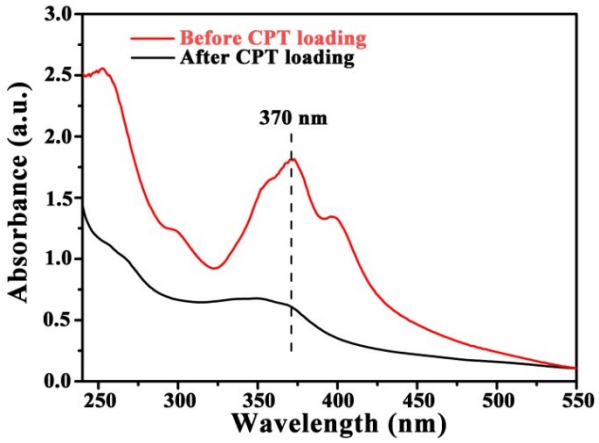

Figure S4. UV/Vis absorption spectra of CPT solution before and after CPT loaded into MOF(Fe)-GOX. For CPT loading, 5 mg CPT was first dissolved in 5 mL dimethylsulfoxide (DMSO), then 5 ml MOF(Fe)-GOX (6 mg/mL) was added into the solution and kept stirring at room temperature for 24 h. The product was isolated by centrifugation and washed thoroughly with deionized water to remove free CPT. The UV/Vis absorbance spectra before and after CPT loading process was shown in **Figure S4,** in which the oberved significant difference at the band of 370 nm solidly comfirms the successfully loading of drug CPT. The drug loading capacity measured by UV/Vis absorption spectroscopy is about 10.6 wt% (106 μg CPT in 1 mg nanoparticles). Drug loading capacity= weight of loaded drug/weight of nanoparticles×100%

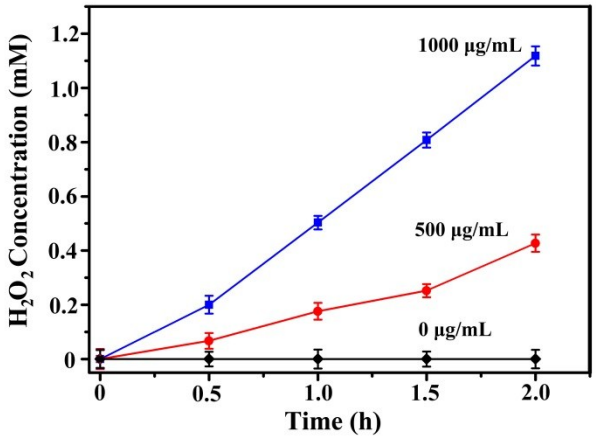

Figure S5. Hydrogen peroxide (H_2O_2) generation profile by MOF(Fe)-GOX catalyzing glucose with different concentrations of 0, 500, and 1000 μg/mL (Reaction 1). The generated H_2O_2 was monitored using a reported molybdate method. Nearly no H_2O_2 was generated in the absence of glucose. In the presence of glucose, substantial H_2O_2 production can be detected and the production rate increases with increasing concentrations of glucose. This result demonstrates the high catalytic ability of GOX on the surface of MOF(Fe).

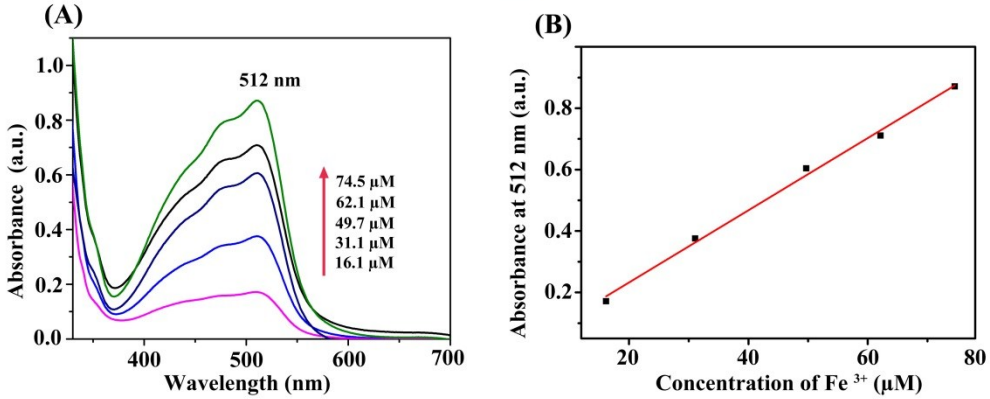

Figure S6. (A) UV-Vis spectra of different concentrations of Fe^{3+} detected using the method of o-phenanthroline. (B) Its corresponding standard curve for Fe^{3+} detection. Fe^{3+} was first reduced to Fe^{2+} by Vitamin C, and then reacted with o-phenanthroline to produce the red complex with maximum absorbance at 512 nm. The absorbance intensity at 512 nm was correlated with the Fe^{3+} concentration. The obtained standard curve can be expressed as y=0.0113x+0.0213, R^2=99.7.

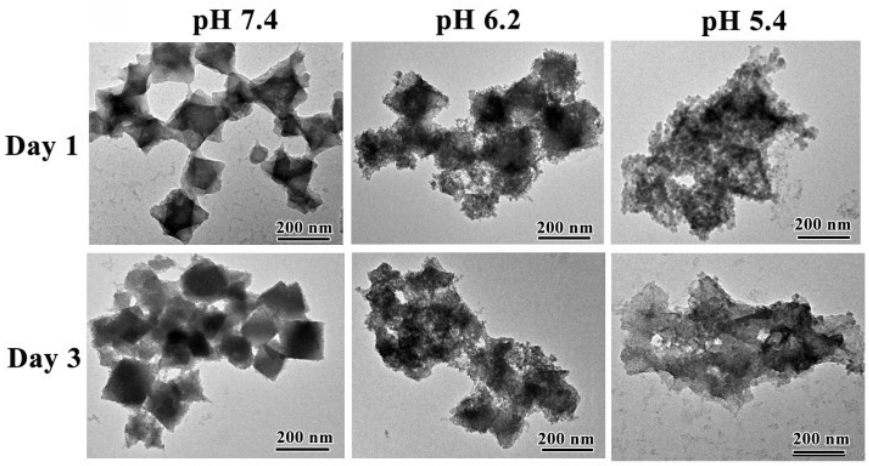

Figure S7. TEM images of MOF(Fe) after 1-day and 3-day degradation under different pH conditions (Reaction 2). It can be seen that the MOF(Fe) exhibits more severe degradation with decreasing pH from under a more acidic environment. Severe MOF(Fe) degradation under acidic condition would facilitate the release of Fe^{3+}. As expected, higher Fe^{3+} concentrations were detected at acidic pH 6.2 and 5.4 as shown in Figure 3. All these proved that MOF(Fe) was can be degraded under acidic condition for the release of Fe^{3+} and drug CPT.

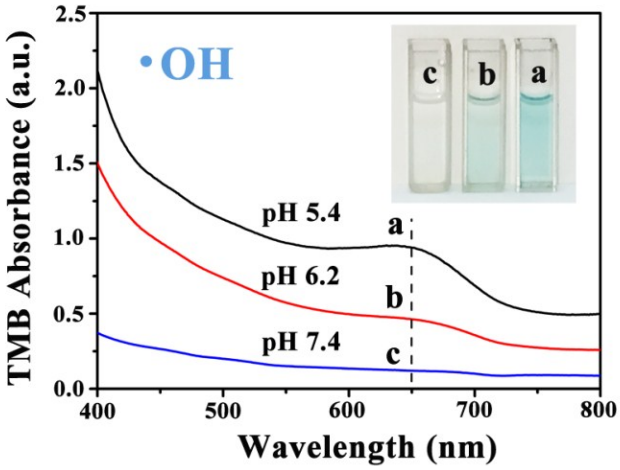

Figure S8 UV-Vis absorbance spectra of ·OH detector (TMB) in the presence of CPT@MOF(Fe)-GOX and glucose at different pH values of 5.4, 6.2, and 7.4 (Reaction 3). The produced ·OH will oxidize colorless TMB to chromogenic TMB cation-free radicals, which have a maximum UV-Vis absorbance at 650 nm. Figure S8 shows that TMB exhibited enhanced absorbance at 650 nm when pH decrease from 6.2 to 5.4 while nearly no absorbance at 650 nm was observed for pH 7.4 case. The corresponding color change in the inset also supports the conclusion of pH-dependent ·OH generation.

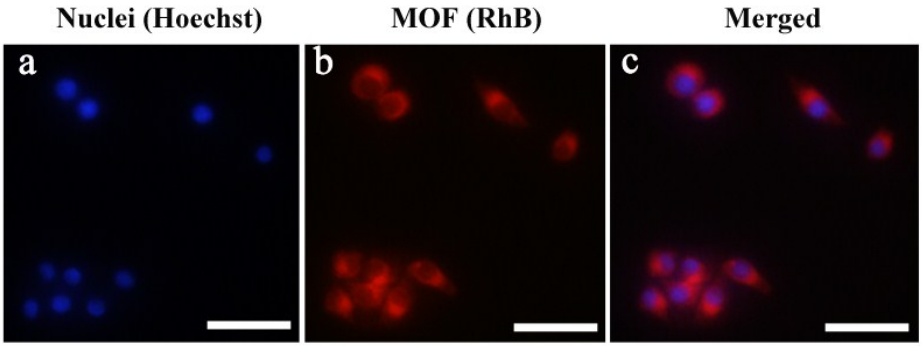

Figure S9. Fluorescence images showing MOF(Fe) internalization in HeLa cells incubated with MOF(Fe) and stained with Hoechst 33342 dye, which shows a blue fluorescence when combined with DNA double strands in the nuclei. Rhodamine B with red fluorescence was employed to label MOF(Fe). As shown in Figure S9, the red fluorescence from RhB can be found in the cytoplasm of HeLa cells around the blue nuclei region, demonstrating the MOF(Fe) have been successfully taken by HeLa cells through endocytosis. Scale bar: 50 μm.

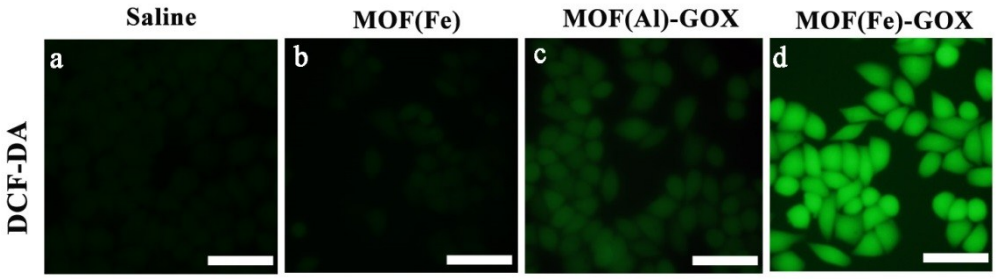

Figure S10. Microscopy images of HeLa cells incubated with Saline, MOF(Fe), MOF(Fe)-GOX, and MOF(Al)-GOX for 4 h, and stained with ROS fluorescent probe (green) DCF-DA. Green fluorescence is observed for the MOF(Fe)-GOX group, indicating a strong ROS (·OH) production whereas no green fluorescence was observed for either Saline or MOF(Fe) group. The weaker green fluorescence observed for MOF(Al)-GOX could be attributed to the generation of H_2O_2 (weaker ROS) according to Reaction 1. Scale bar: 50 μm.

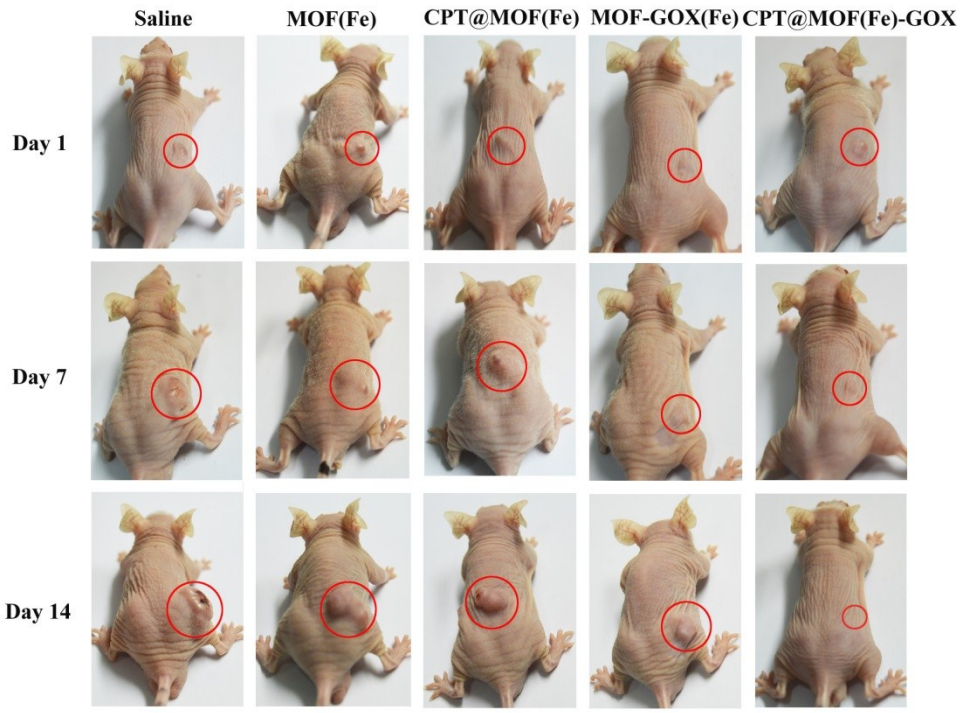

Figure S11. Digital photos of HeLa tumor-bearing mice after different treatments for 14 days. For saline and MOF(Fe) groups, the tumor volume of mice increased rapidly in 14 days. When treated with CPT@MOF(Fe) or MOF(Fe)-GOX, the mice tumor exhibits a slower growth rate as the result of either chemotherapy or starvation/ROS-medicated therapy. In contrast, a remarkable synergistic effect with minimum tumor growth rate due to a cascade reaction activated Starvation/ROS-mediated/Chemo therapy for CPT@MOF(Fe)-GOX group (see the rightmost column) was observed.

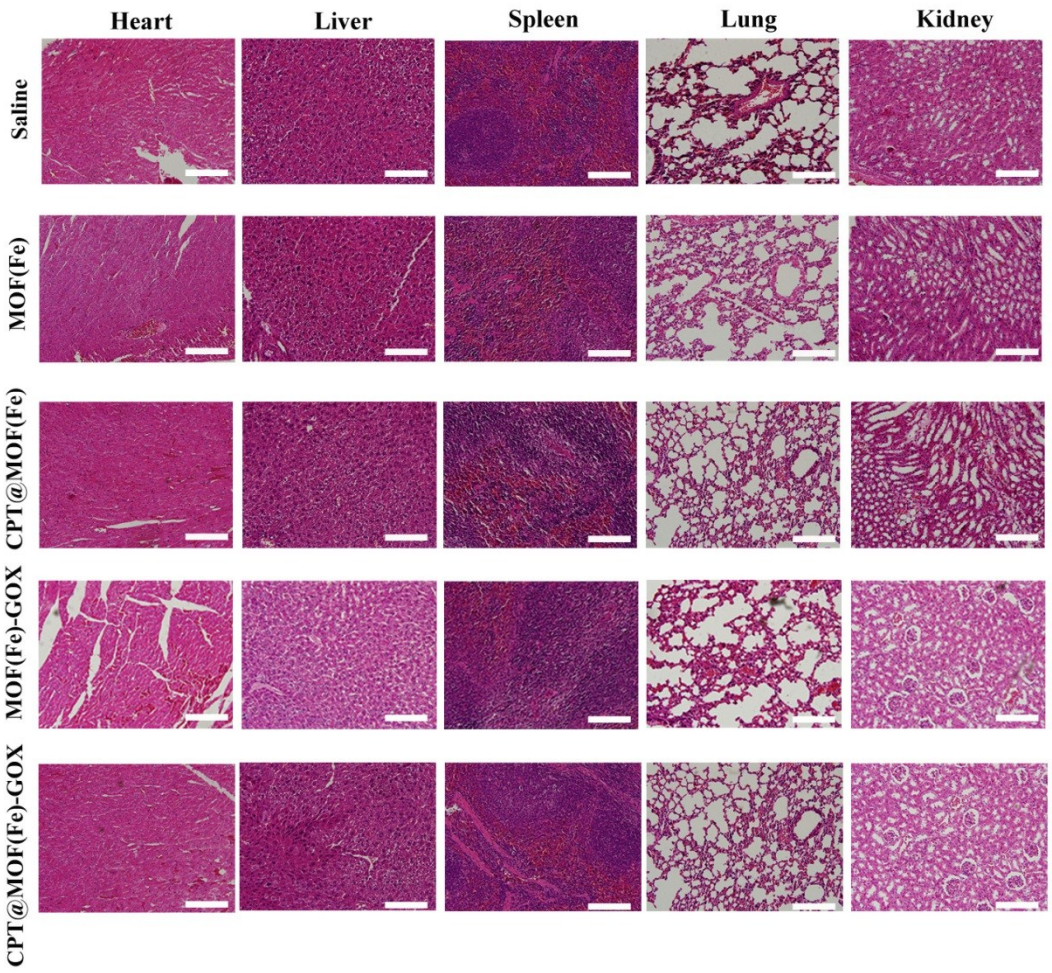

Figure S12. H&E staining of heart, liver, spleen, lung and kidney of the mice from the five groups. Compared with the saline group, no significant morphological change in H&E images of the major organs in different groups was observed demonstrating the high biosafety and biocompatibility of our platform during the therapeutic process. Scale bar: 200 μm.

References

[1] Taylor-Pashow, K. M.; Della, R. J.; Xie, Z.; Tran, S.; Lin, W. Postsynthetic modifications of iron-carboxylate nanoscale metal-organic frameworks for imaging and drug delivery. *J. Am. Chem. Soc.* **2009**, *131*, 14261-14263.

[2] Zhang, Z.; Li, X.; Liu, B.; Zhao, Q.; Chen, G. Hexagonal microspindle of NH_2-MIL-101(Fe) metal-organic frameworks with visible-light-induced photocatalytic activity for the degradation of toluene. *Rsc Adv.* **2015**, *6*, 4289-4295.

[3] Barbosa, A. D. S.; Julião, D.; Fernandes, D. M.; Peixoto, A. F.; Freire, C.; Castro, B. D.; Granadeiro, C. M.; Balula, S. S.; Cunha-Silva, L. Catalytic performance and electrochemical behaviour of metal–organic frameworks: Mil-101(Fe) versus NH_2-MIL-101(Fe). *Polyhedron* **2016**.